

SUPPORTING INFORMATION

Conformational thermodynamics guided structural reconstruction of bio-molecular fragments

Samapan Sikdar ¹, J. Chakrabarti ^{1,2 *} and Mahua Ghosh ^{1 *}

¹

Department of Chemical, Biological And Macromolecular Sciences, S. N. Bose National
Centre for Basic Sciences, Sector III, Block JD, Salt Lake, Kolkata 700098, INDIA

²

Also at Unit of Nanoscience and Technology-II and The Thematic Unit of Excellence on
Computational Materials Science, S. N. Bose National Center for Basic Sciences, Sector III,
Block JD, Salt Lake, Kolkata 700098, INDIA

*Corresponding authors:

E.mail: jaydeb@bose.res.in and mahuaghosh@bose.res.in

Table S1. The solvent accessible surface area (SASA) of the ensemble averaged conformations of model A, model B, 2Ca²⁺-TnC and 4Ca²⁺-TnC.

TnC	SASA (Å ²)
Model A	9374
Model B	9375
2Ca ²⁺ -TnC	9842
4Ca ²⁺ -TnC	9838

Table S2. The backbone conformational entropy change of central linker residues in model B compared to model A.

Residues	$T\Delta S_i^{\text{conf}}$ (kJ/mol)
M81	0.84
V82	0.89
R83	2.23
Q84	3.89
M85	2.05
K86	0.26
E87	0.69
D88	~0
A89	-0.94
K90	-3.71
G91	~0
K92	-4.39
S93	-4.68
E94	-3.32
E95	1.28
E96	1.91

Table S3. Homologous sequences with variable similarity from PDB compared to the query sequence of “QMKE^DA^KG^KS^EEE” corresponding to the missing fragment of TnC. The secondary structures, like helix (H, G), turn (T), bend (S) and beta strand (B, E) are assigned through DSSP.

PDB id-chain id	Sequence	Secondary structure
2I0Z-A	QMKE ^D -----	HHTTS-----
1AYZ-A	-MKED-----	-HHHS-----
4HD5-A	-MKED-----	-EETT-----
3BAT-A	-MKED-----	-HHHH-----
1Y6Z-A	-MKED-----	---TT-----
1M1S-A	----DAKGKS---	-----TT-EE---
3HQ2-A	----AKGKS---	-----HHHTT--
3BDU-A	----AKGK---	-----EE-----
3DDL-A	-----KSEEE	-----HHHHT
2I6X-A	-----KSEEE	-----S-HHH
3LMZ-A	-----KSEEE	-----SHHH
3ZN3-A	-----KSEEE	-----HH---
2Z4T-A	-----KSEEE	-----HHHH
4H0P-A	-----SEEE	-----EEEE
4QAN-A	-----SEEE	-----SSH
1Y0U-A	-----SEEE	-----HHH
1CFD-A	-----SEEE	-----SHHH
3GTD-A	-----SEEE	-----HHH
3RFU-A	-----SEEE	-----EEEE
2A5Y-A	QMKE ^D -----	HHHHH-----
1BJ8-A	-MKEDGKG----	-EESSS-----
2BFH-A	-MKEDG-----	-E-TTS-----
1K3B-B	-MKED-----	---SS-----
1ITF-A	-MKED-----	-HHHH-----
4ACJ-A	-MKED-----	-SSSE-----
3UNF-K	-MKED-----	-EETT-----
3LFL-A	-MKED-----	-HHHH-----
4XKK-A	-MKED-----	-E-GG-----
1KCM-A	-MKED-----	-TGGG-----
1AQU-A	-MKED-----	-HHH-----
4OA6-A	-MKED-----	-S-----
1VK1-A	--KEDAK-----	--HHHHH-----
2JI5-A	--KEDAK-----	--HHHHT-----

1WZN-A	--KEDAK-----	--HHT-S-----
3RP9-A	--KEDAK-----	---HHHH-----
2EQU-A	---EDAKG-----	---GGGT-----
1NI4-B	---EDAKG-----	---HHHHH-----
1E8X-A	---EDAK-----	---HHHH-----
3R3J-A	-----KGKSE--	-----TT--H--
2ODR-A	-----KGKSE--	-----HHHHH--
4BFR-A	-----GKSEEE	-----TB-HHH
1N1B-A	-----SEEE	-----HHH
1EF1-C	-----RSEEE	-----TGGGG
1AD6-A	-----KSEEE	-----HHHHH
4BC6-A	-----KSEEE	-----SHHH
1LFH-A	-----KSEEE	-----S-HHH
1LFI-A	-----KSEEE	-----S-TTH
2CRK-A	-----KSEEE	-----HHHH
3BJU-A	-----KSEEE	-----S-HHH
1M1E-B	-----SEEE	-----HHHH
1Y8Q-A	-----SEEE	-----HHH
3EVR-A	-----SEEE	-----HHHH
4OY4-A	-----SEEE	-----HHH
3S9V-A	-----SEEE	-----BHHH
2F05-A	-----SEEE	-----HHH

Table S4. The destabilized and disordered residues of 2Ca²⁺-TnC with respect to model A (set A).

Residues	ΔG_i^{conf} (kJ/mol)	$T\Delta S_i^{conf}$ (kJ/mol)
F28	0.91	1.80
Q50	1.39	8.47
F77	0.74	1.01
M80	0.42	3.30
M81	0.17	2.36
D88	0.39	3.22
R102	1.35	1.19
T124	0.67	2.03
E126	1.57	6.04
H127	0.52	3.62
V128	1.87	1.32
D132	0.52	0.28
M157	2.20	7.57

V160	1.11	5.14

Table S5. Comparison of inter-helical angles, $\theta_{i,j}$ between helices i and j of the ensemble averaged conformations of model A, model B and the constructed models from Rosetta, RaptorX, PHYRE2 and ModLoop.

ANGLE	Model A	Model B	Rosetta model	RaptorX model	PHYRE2 model	ModLoop model
$\theta_{a,b}$	144°	138°	137°	129°	137°	129°
$\theta_{c,d}$	114°	134°	148°	133°	148°	128°
$\theta_{e,f}$	160°	146°	102°	108°	102°	94°
$\theta_{g,h}$	141°	128°	106°	102°	106°	100°

Figure Captions

Fig S1. Initial apo-TnC models (a) model A and (b) model B. (c) RMSD and (d) RMSF of model A (black), model B (red), 2Ca²⁺-TnC (green) and 4Ca²⁺-TnC (blue).

Fig S2. The equilibrium probability distributions of backbone dihedral angles, $P_i^A(\phi)$ (black solid line), $P_i^A(\psi)$ (black dashed line) of (a) K86, (b) E87, (c) D88, (d) A89 in model A and similarly $P_i^B(\phi)$ (black solid line), $P_i^B(\psi)$ (black dashed line) of (e) K86, (f) E87, (g) D88, (h) A89 in model B. The insets represent the corresponding ϕ - ψ scatter-plots, where helix conformation is shown in black dots.

Fig S3. The equilibrium probability distributions of backbone dihedral angles, $P_i^A(\phi)$ (black solid line), $P_i^A(\psi)$ (black dashed line) of (a) K92, (b) S93, (c) E94 and (d) E95 in model A and similarly $P_i^B(\phi)$ (black solid line), $P_i^B(\psi)$ (black dashed line) of (e) K92, (f) S93, (g) E94 and (h) E95 in model B. The insets represent the corresponding ϕ - ψ scatter-plots, where helix conformation is shown in black dots.

Fig S4. The distribution of (a) inter-domain distance $P(d_{N-C})$, (b) inter-domain angle $P(\theta_{N-C})$ and (c) radius of gyration $P(R_g)$ calculated from the ensemble of model A (black solid line) and that of model B (gray dashed line). (d) The distribution of $M85_{C\alpha} - E95_{C\alpha}$ distances, $P(d_{M85-E95}^{C\alpha})$ in the NMR, PDB id 1TNW (black solid line) and the simulated (gray dashed line) ensemble of 4Ca²⁺-TnC.

Fig S5. Homology based models of apo-TnC from (a) Rosetta using PDB template 1TOP, (b) RaptorX using PDB template 1NCX, (c) ModLoop using PDB template 1YV0. The central linker residues M85-E95 are coloured in black.

Fig S6. (a) RMSD plot of ModLoop model. (b) The distribution of radius of gyration $P(R_g)$ calculated from the ensemble of ModLoop model. Conformational thermodynamic changes in ModLoop model with respect to model B, illustrating (c) stabilized (green) and destabilized (yellow) residues (d) ordered (green) and disordered (yellow) residues. (e) The energy minimized $2\text{Ca}^{2+}\text{-TnC-TnI}$ docked complex where the destabilized and disordered interfacial residues of $2\text{Ca}^{2+}\text{-TnC}$ with respect to the ModLoop model are shown in red.

Fig S7. The energy minimized $2\text{Ca}^{2+}\text{-TnC-TnI}$ docked complex where the destabilized and disordered interfacial residues of $2\text{Ca}^{2+}\text{-TnC}$ with respect to the model A are shown in red.

Fig S8. The ordered (green) and disordered (yellow) residues (a) in the C-terminal domain of $2\text{Ca}^{2+}\text{-TnC}$, (b) in the N-terminal domain of $4\text{Ca}^{2+}\text{-TnC}$, (c) in the C-terminal domain of $4\text{Ca}^{2+}\text{-TnC}$ with respect to model B.

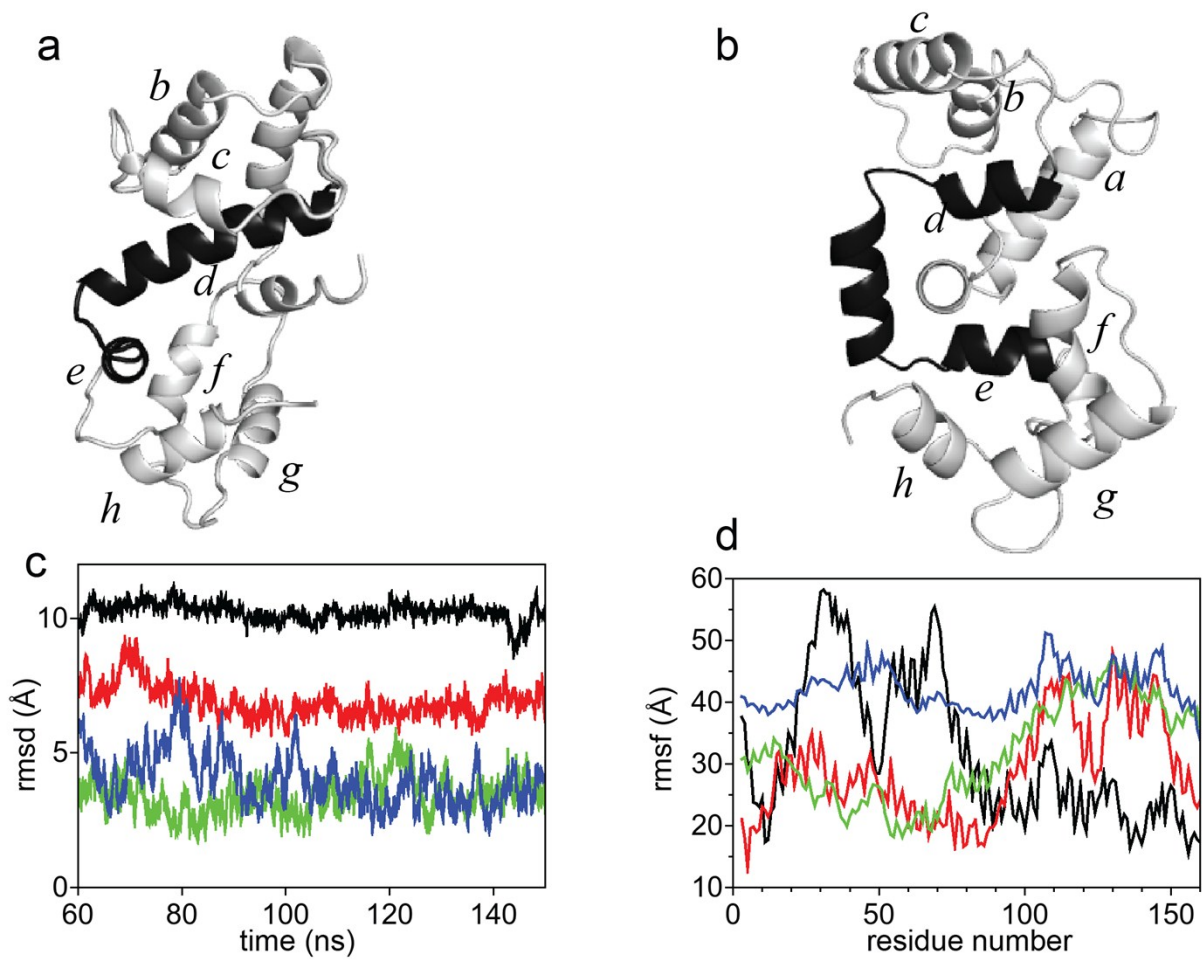


Fig S1.

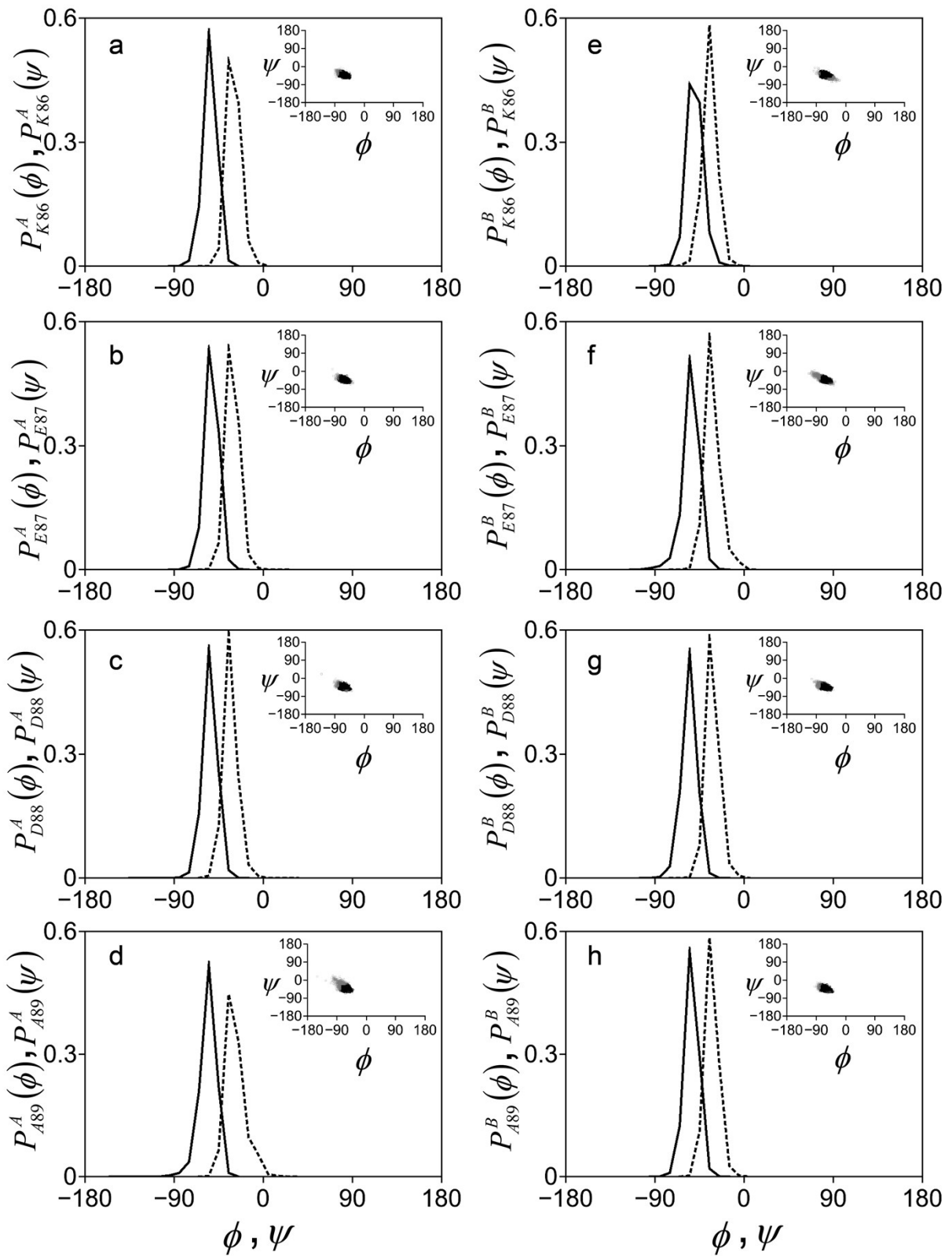


Fig S2.

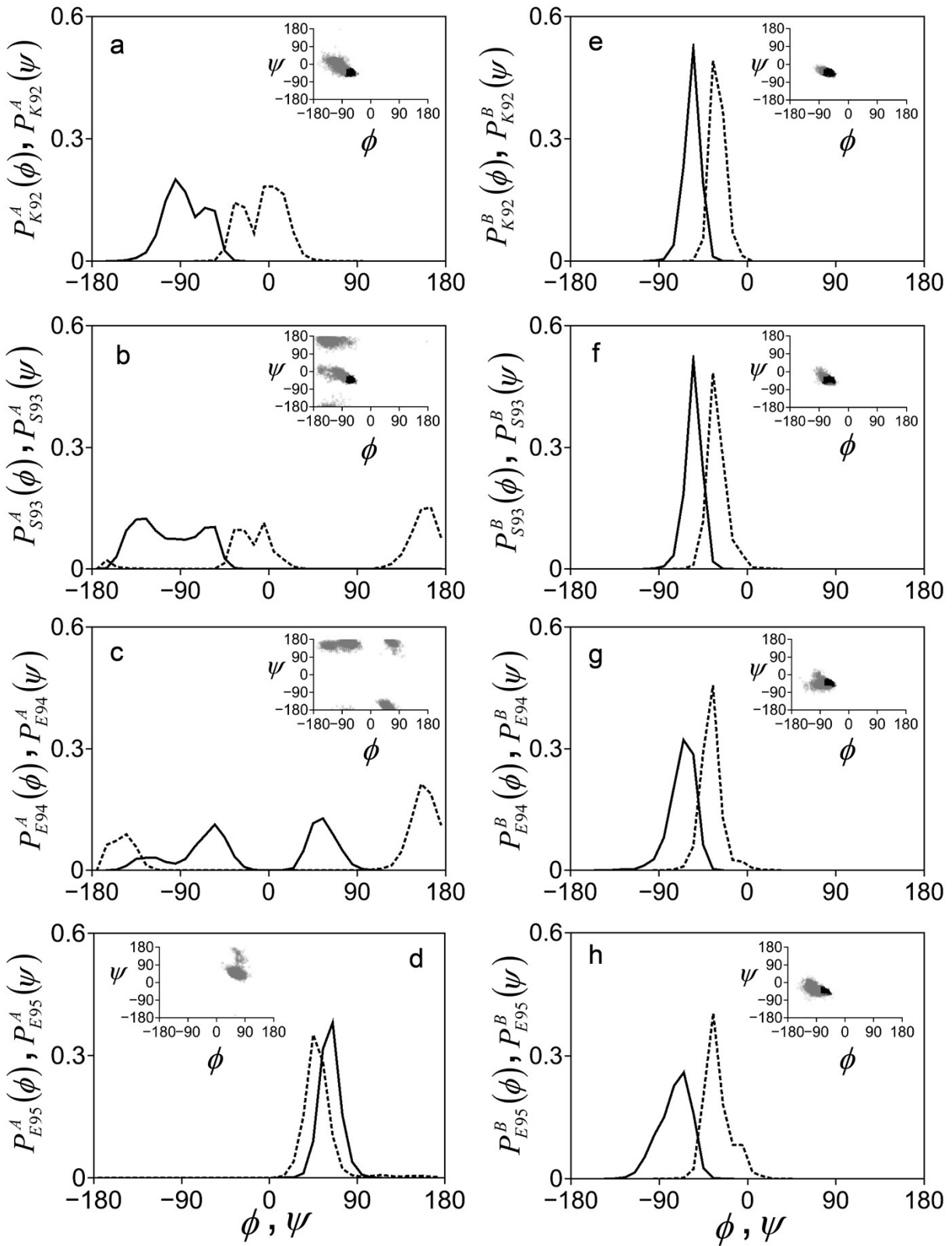


Fig S3.

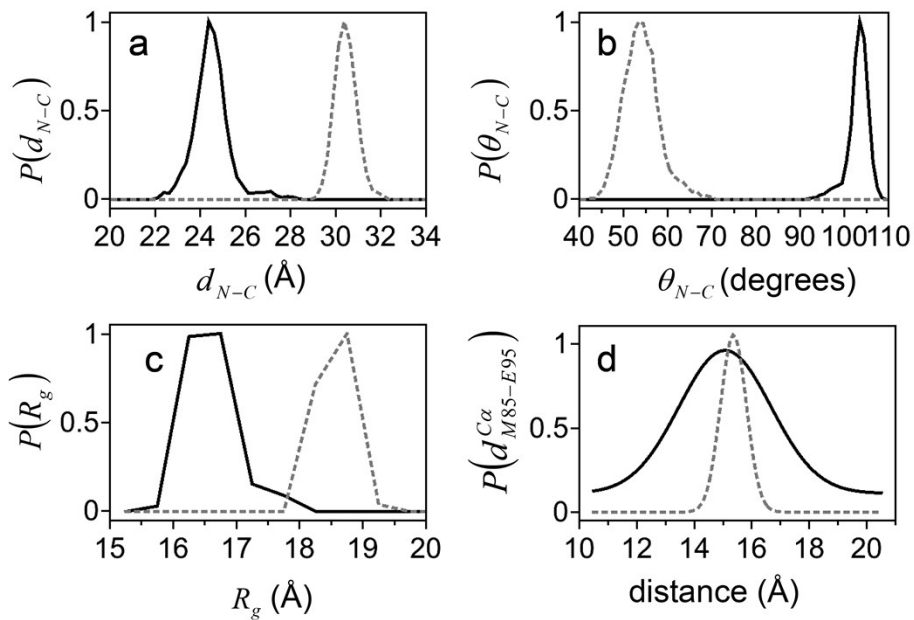


Fig S4.

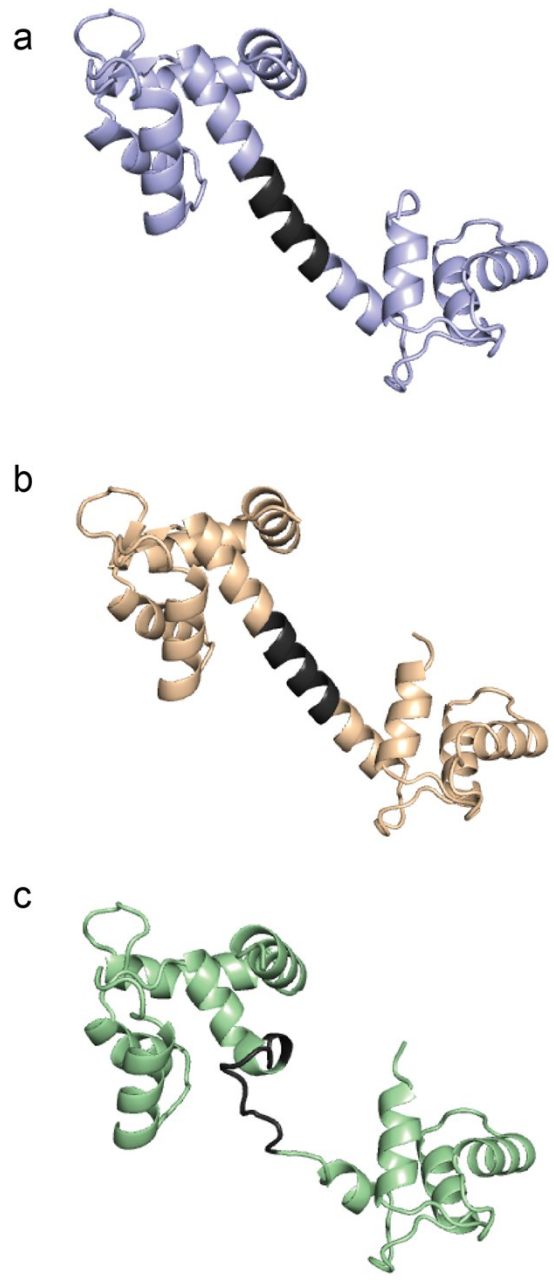


Fig S5.

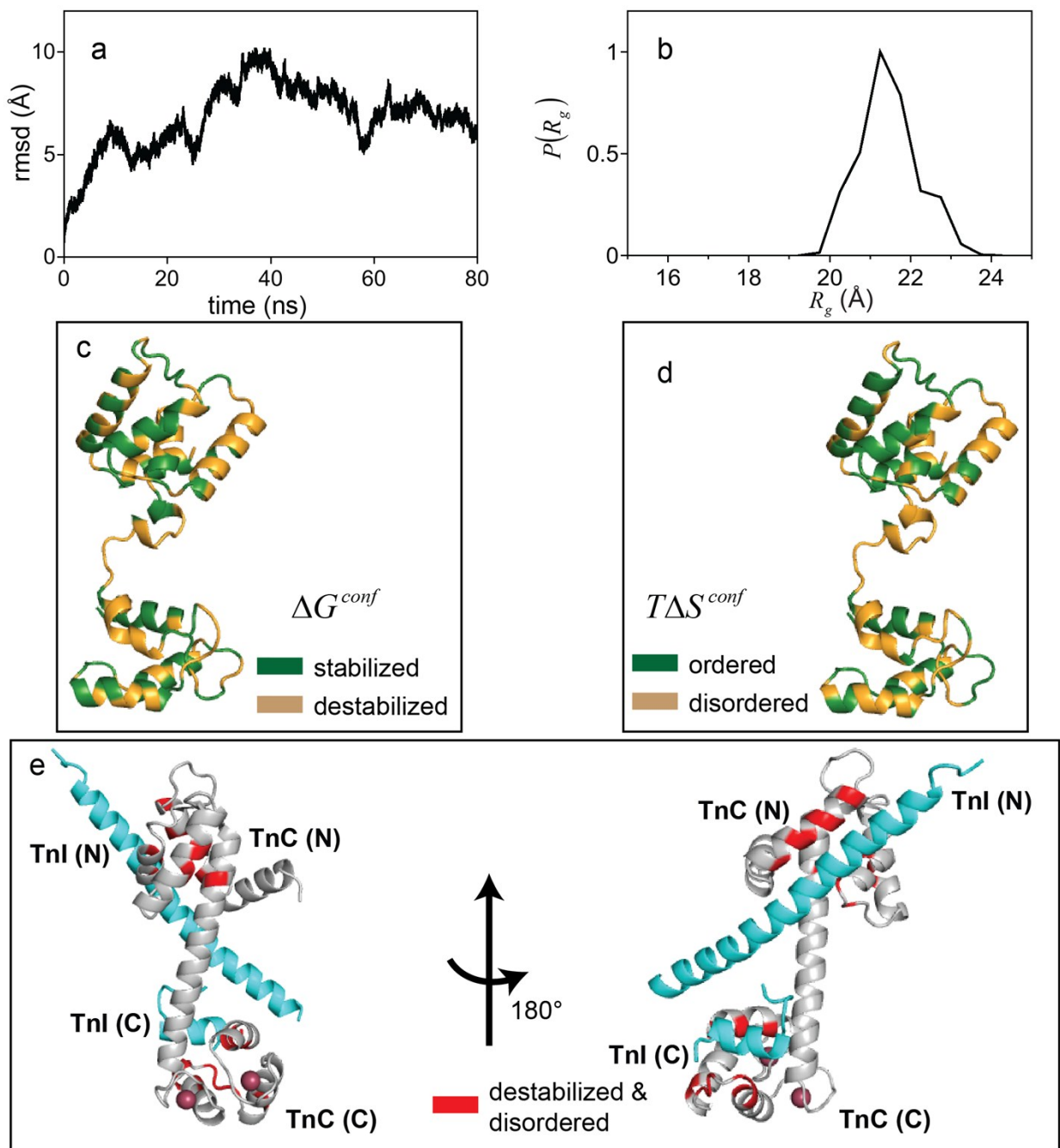


Fig S6.

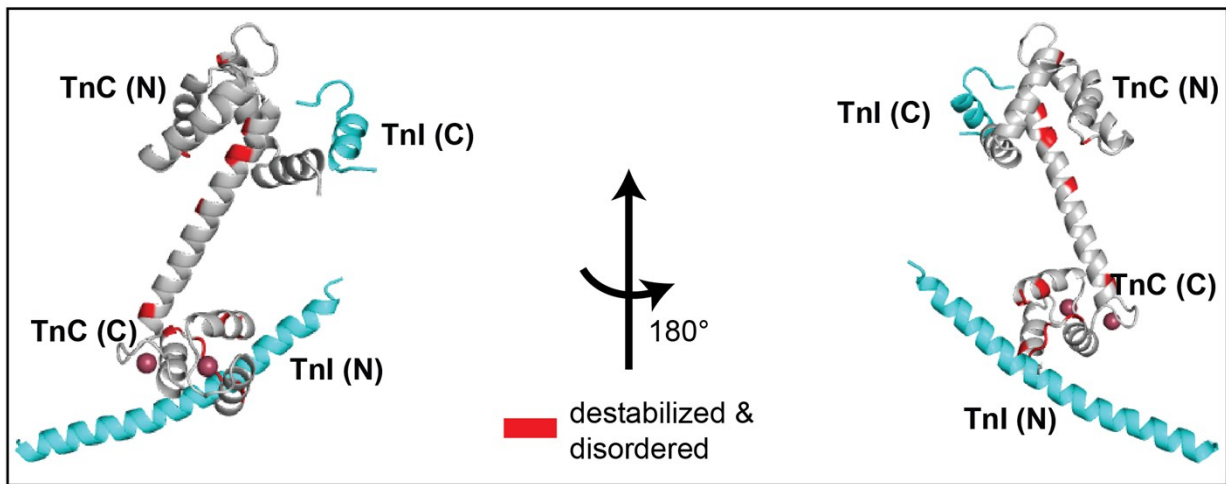


Fig S7.

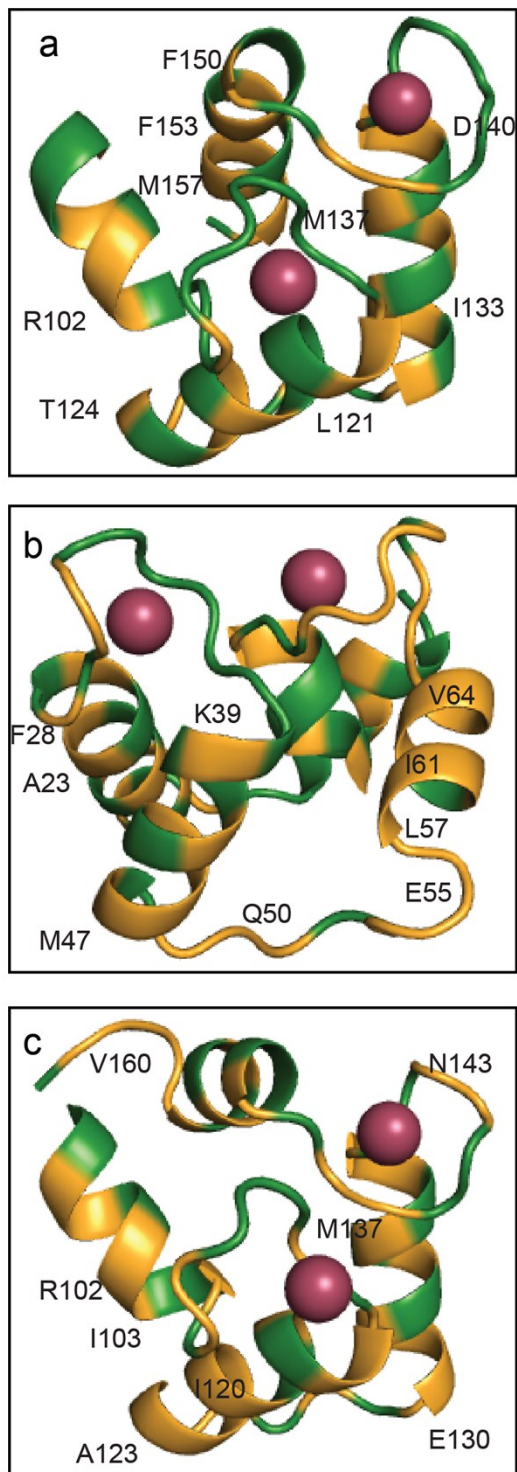


Fig S8.